Electronic Supplementary Material (ESI) for Journal of Materials Chemistry B.

Boosting immunotherapy of triple negative breast cancer through the synergy of mild PTT and Fe-doped organo-silica nanoparticles.

Ben Yang[1, 2], Hui Fu[2], Ronghua Kong[2], Gang Zheng[2], Xihong Wang[2], Yang Dong[2, *], and Zhenlin Yang[3, 4, *]

[1] Shandong University Cancer Center, Jinan, Shandong, 250012 China;

[2] Department of Breast Surgery, Shandong Cancer Hospital and Institute, Shandong First Medical University and Shandong Academy of Medical Sciences, Jinan, Shandong, 250117 China;

[3] Cheeloo College of Medicine, Shandong University, Jinan, Shandong, 250012 China;

[4] Department of Thyroid and Breast Surgery, Binzhou Medical University Hospital, Binzhou, Shandong, 256603, China；

Corresponding authors:

Prof. Zhenlin Yang, Cheeloo College of Medicine, Shandong University, Jinan, Shandong, 250012 China; Department of Thyroid and Breast Surgery, Binzhou Medical University Hospital, Binzhou, Shandong, 256603, China

E-mail: ikb0607@163.com

Prof. Yang Dong, Department of Breast Surgery, Shandong Cancer Hospital and Institute, Shandong First Medical University and Shandong Academy of Medical Sciences, Jinan, Shandong, 250117 China;

E-mail: sdxtdongyang@163.com

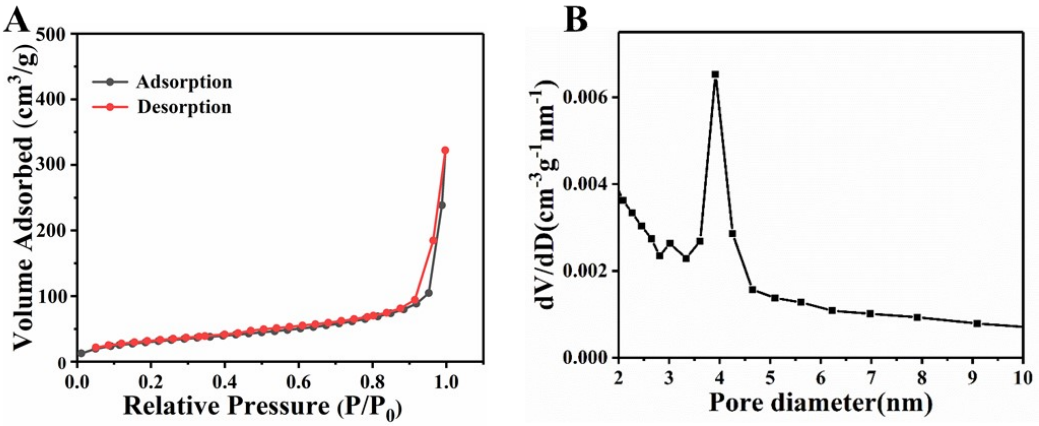

Figure S1. (A) N_2 adsorption-desorption isotherms and (B) pore-size distributions of MON.

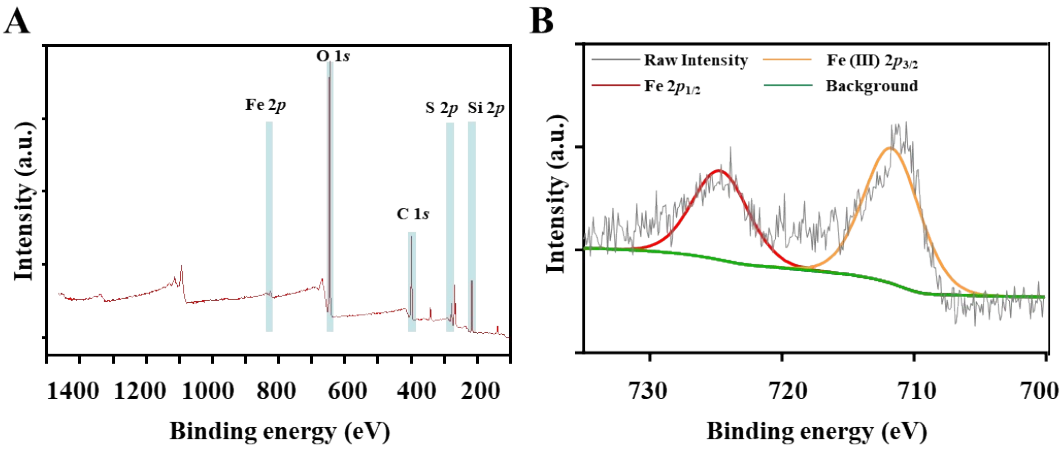

Figure S2. (A) XPS survey spectrum of HMONs. (B) Local XPS spectra for the Fe elementary analyses of IMOFHs.

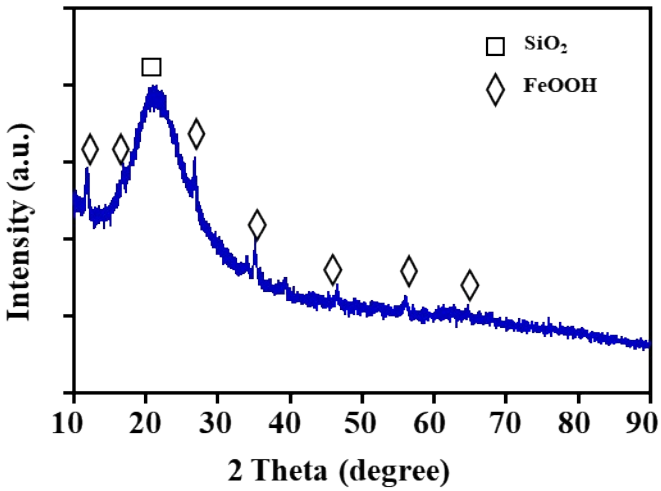

Figure S3. XRD patterns of MOF. Square symbol indicated amorphous peak of SiO_2 (PDF#81-0066), while diamond symbol indicated the characteristic peaks of FeOOH (PDF#70-0714)

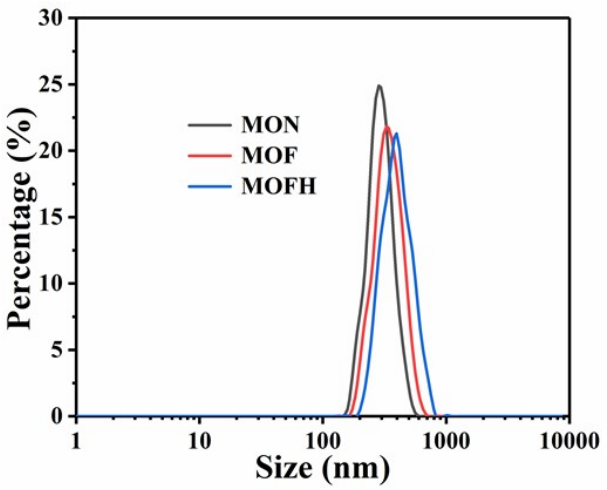

Figure S4. Particle size distribution of MON, MOF and MOFH.

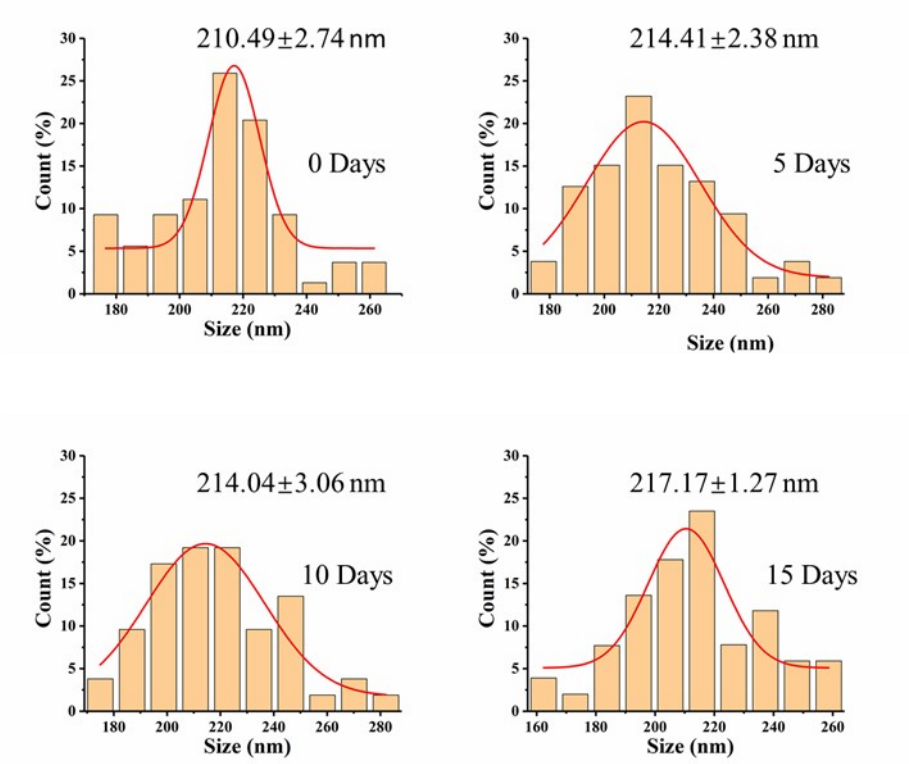

Figure S5. Particle size change of MOFH dispersed in PBS buffer for different time.

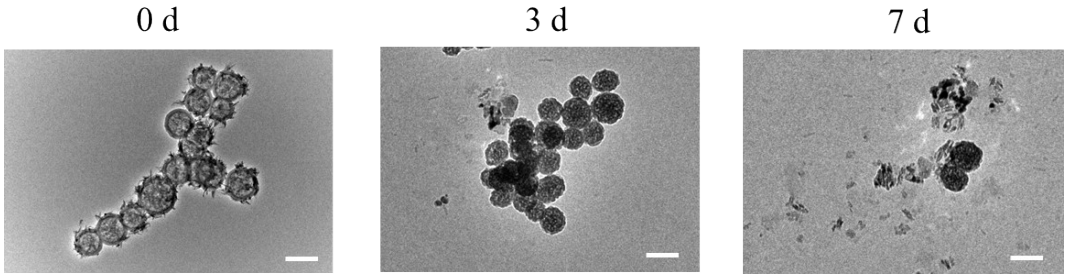

Figure S6. TEM images of MOFH after degradation in PBS (pH = 6.5) and the presence of GSH (10 mM) for 0, 7, and 14 days. Scale bars: 200 nm.

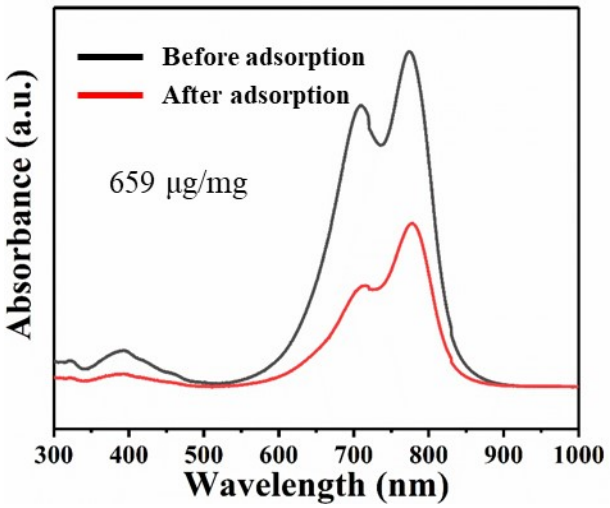

Figure S7. UV-vis absorption spectra of ICG solutions before and after the incubation with MOFH.

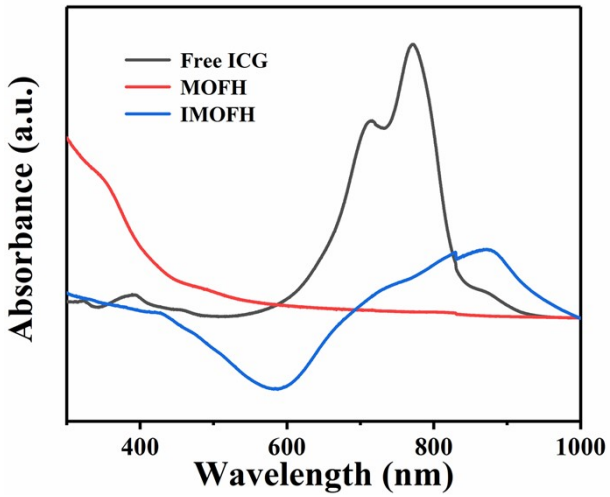

Figure S8. UV-vis absorption spectra of Free ICG, MOFH, and IMOFH.

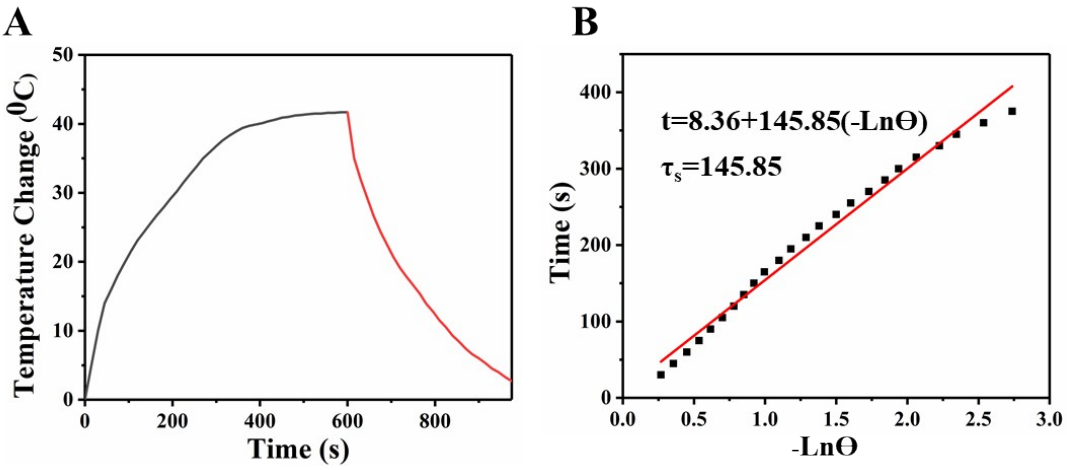

Figure S9. (A) The heating and cooling curve of the aqueous solution of IMOFH after NIR radiation. (B) The cooling period versus negative natural logarithm of driving force temperature.

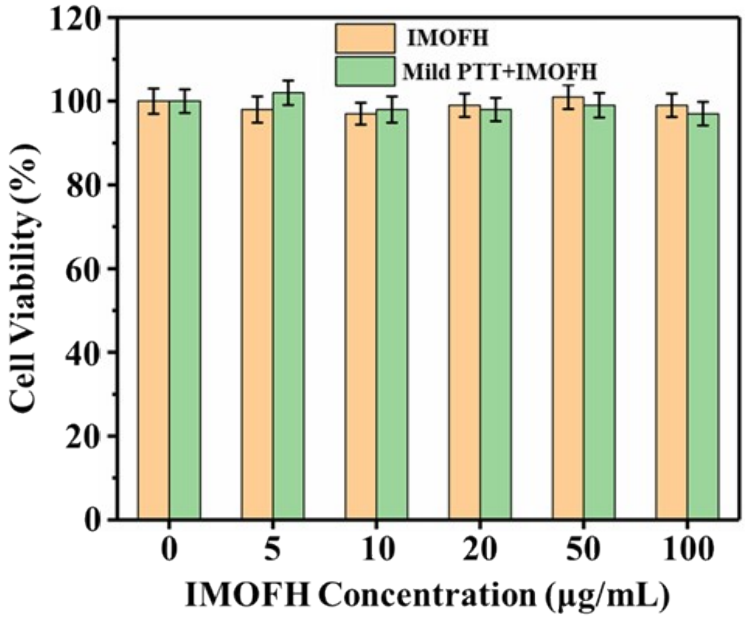

Figure S10. LO2 cells viability incubated with IMOFH with or without mild PTT.

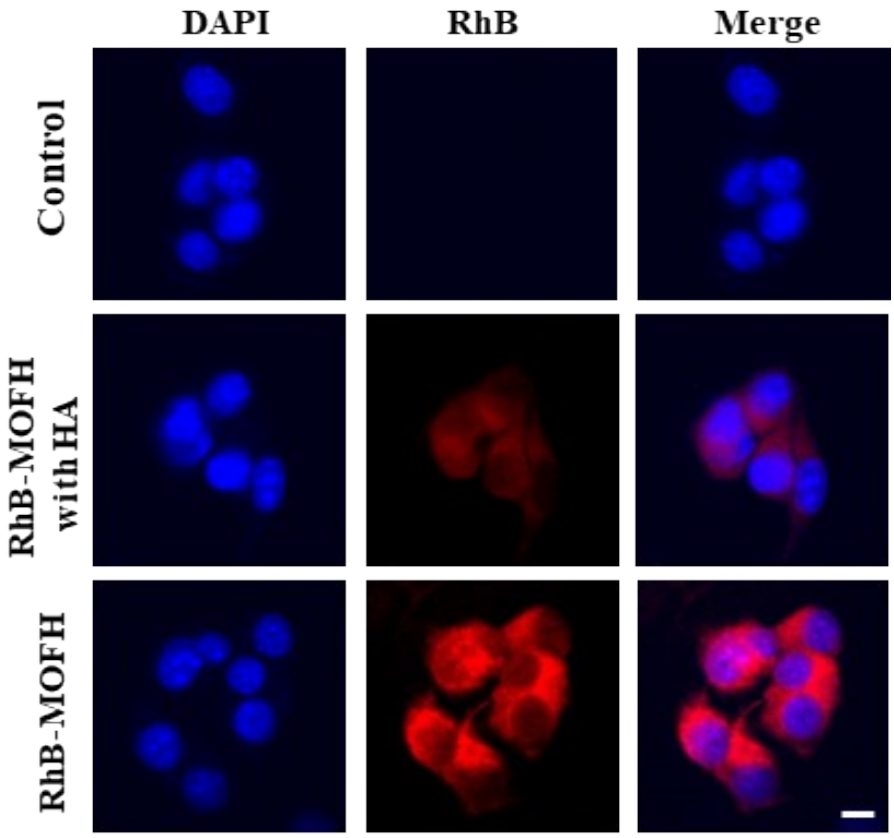

Figure S11. Confocal laser scanning microscopy (CLSM) of 4T1 intracellular uptake of Rhodamine B (RhB)-loaded MOFH with or without HA pre-incubated. Scale bar = 20 μm.

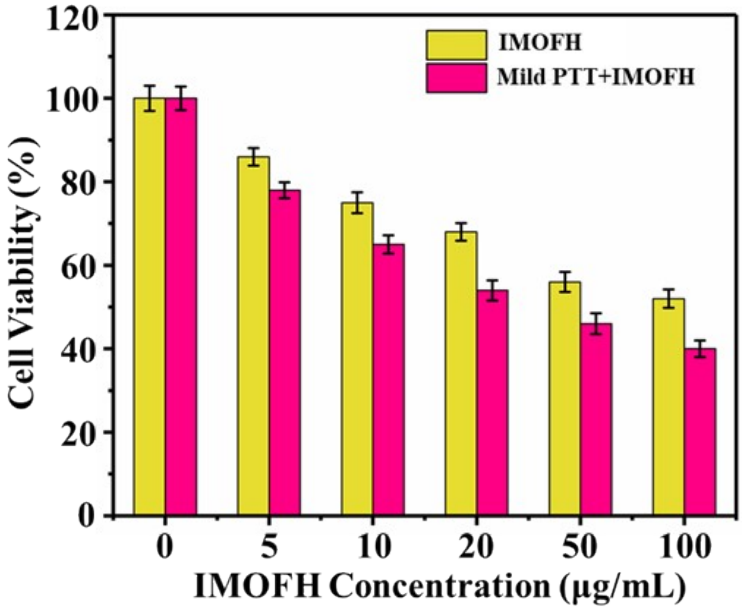

Figure S12. 4T1 cells viability incubated with IMOFH with or without mild PTT.

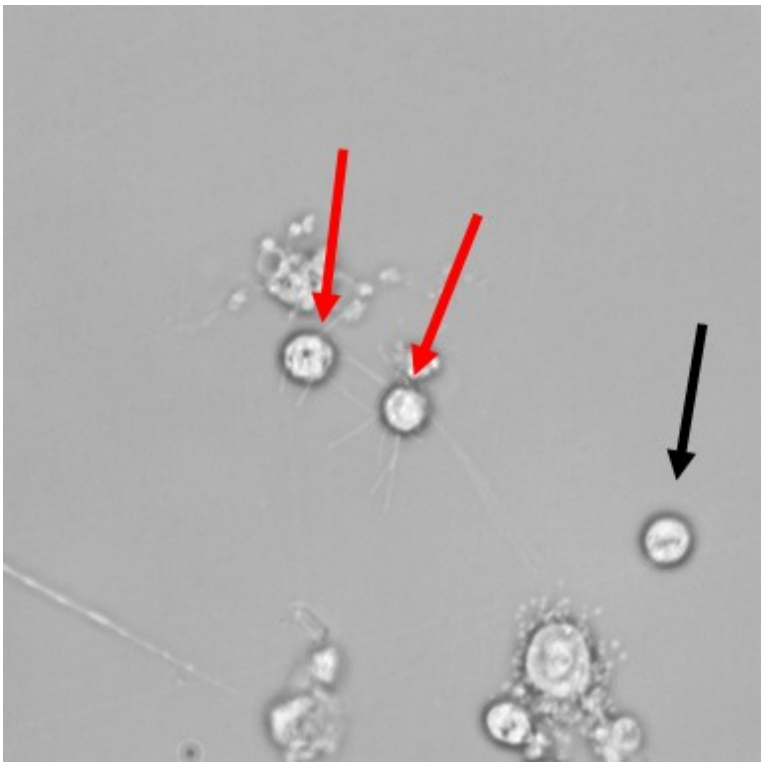

Figure S13. The photos of bone marrow derived dendritic cells (BMDCs) stimulated with tumor-related antigen. Red arrows: matured DCs; Black arrow: inactivated DCs.

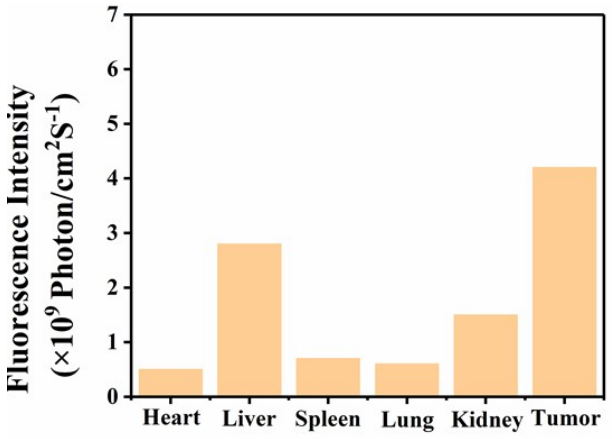

Figure S14. Quantification the mean fluorescence in organ and tumor regions by *in vivo* imaging.

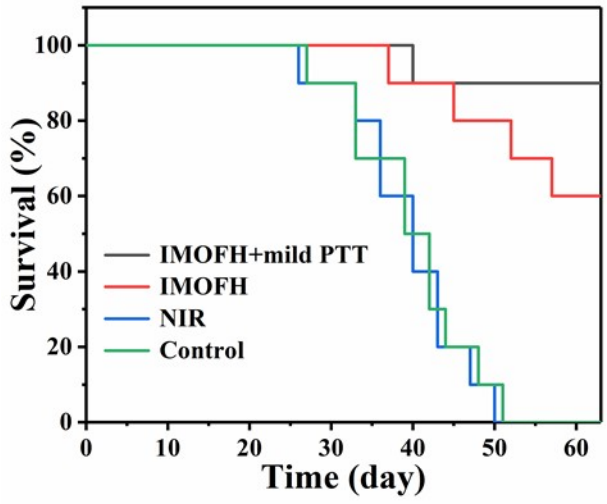

Figure S15. The survival curve of tumor-bearing mice in response to different treatments.

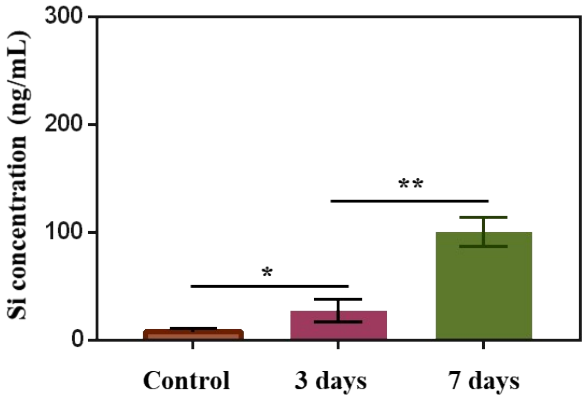

Figure S16. Si concentration in digested tumor suprnatant for 0 (control), 7, and 14 days. All data are presented as the mean ± SD; n = 3. *P < 0.05, **P < 0.01.